



Article

Effect of Metallic and Non-Metallic Additives on the Synthesis of Fullerenes in Thermal Plasma

Anna Mária Keszler¹, Éva Kováts², Eszter Bódis¹ , Zoltán Károly^{1,*}  and János Szépvölgyi¹

¹ Research Centre for Natural Sciences, Institute of Materials and Environmental Chemistry, Magyar Tudósok krt. 2., H-1117 Budapest, Hungary; keszler.anna.maria@ttk.hu (A.M.K.); bodis.eszter@ttk.hu (E.B.); szepvolgyi.janos@ttk.hu (J.S.)

² Institute for Solid State Physics and Optics, Wigner Research Centre for Physics, Konkoly-Thege Miklós u. 29-33., H-1121 Budapest, Hungary; kovats.eva@wigner.mta.hu

* Correspondence: karoly.zoltan@ttk.hu

Abstract: The effect of metallic (Fe, Cu, Co, Ni, Ti) and non-metallic additives (Si, B) on the formation of fullerenes from graphite powders was studied in radiofrequency (RF) thermal plasma. The main component of the synthesized fullerene mixtures was C₆₀, but higher fullerenes (C₇₀, C₈₂, and C₈₄) could be detected as well. Fe and Cu additives increased the fullerene content in the soot. In contrast, the fullerene formation decreased in the presence of Ti, Si, and B as compared to the synthesis without additives. However, Ti and B addition enhanced the formation of higher fullerenes. We provide experimental evidence that decreasing the reactor pressure results in a lower yield of fullerene production, in accordance with thermodynamic calculations and numerical simulations published earlier. In the presence of titanium, a significant quantity of TiC was also formed as a by-product. The fullerene mixture synthesized with boron additives showed higher stability during storage in ambient conditions as compared to other samples.

Keywords: fullerenes; plasma synthesis; emission spectra; HPLC



Citation: Keszler, A.M.; Kováts, É.; Bódis, E.; Károly, Z.; Szépvölgyi, J. Effect of Metallic and Non-Metallic Additives on the Synthesis of Fullerenes in Thermal Plasma.

Condens. Matter **2022**, *7*, 44. <https://doi.org/10.3390/condmat7030044>

Academic Editor: Levan Chkhartishvili

Received: 27 May 2022

Accepted: 28 June 2022

Published: 30 June 2022

Publisher's Note: MDPI stays neutral with regard to jurisdictional claims in published maps and institutional affiliations.



Copyright: © 2022 by the authors. Licensee MDPI, Basel, Switzerland. This article is an open access article distributed under the terms and conditions of the Creative Commons Attribution (CC BY) license (<https://creativecommons.org/licenses/by/4.0/>).

1. Introduction

Since their discovery by Kroto and coworkers [1], much research work has been reported on fullerenes. Due to their special electronic, mechanical, and photophysical properties, they have potential in a various applications including organic electronics [2], solar energy utilization [3], energy storage [4,5], as sensor materials [6], and biomedicine [7–9]. The high cost and the insufficient availability of fullerenes raise difficulties for their broader applications [10]. The development of large-scale and low-cost production technologies of fullerenes seems to be a goal of outstanding importance both in scientific and practical terms [11–13]. Any study aiming to contribute towards enhancing the production of fullerenes will invariably promote advancements in its applications [14].

Various methods have been used to produce fullerenes from carbon vapors, such as arc discharge plasma [15–18], solar flux [19], laser vaporization [20], or RF or hybrid (RF/DC) thermal plasmas [21–23]. Although the methods based on graphite vaporization and burning hydrocarbon in a fuel-rich flame [24–27] are the most frequently used, a few other interesting methods have been also reported [28–31]. These show selectivity for a given number of carbon fullerenes and are based on planar polycyclic aromatic hydrocarbon precursor molecules.

As was shown in earlier studies, inductively coupled radiofrequency (RF) thermal plasma offers favorable conditions for fullerene synthesis [32,33]. Numerous papers have been published about the advantageous and disadvantageous effects of different additives and impurities on fullerene formation. It is generally accepted that, in the synthesis of fullerenes, the presence of other elements should be avoided, because they can bind to the

free C bond and inhibit the closure of the cluster. At the same time, a positive influence of the catalysts has been found [34,35].

Wang et al. [34] found that Si addition to the starting carbon powder enhanced the C₆₀ formation. In the absence of Si, fullerene formation could not be detected in their plasma system.

Laser evaporation of the mixture of graphite and BN resulted in the formation of fullerenes and boron-containing analogues such as C₅₉B and C₅₄B₆ [36]. In DC plasma, however, Lange et al. [37] found a decrease in fullerene content in the presence of boron.

Iron is a widespread catalyst in carbon nanotube (CNT) synthesis. It is obvious to suppose its favorable effect on fullerene synthesis, as well. Cota-Sanchez et al. [35] confirmed these expectations in an RF plasma system. In some cases, they observed the formation of CNTs as well. Fullerenes and CNTs were also found in the presence of Ni catalyst [38]. A 2D numerical model has been developed to describe the continuous synthesis of fullerenes in the presence of Ni particles in induction thermal plasma [39].

Among the various operating parameters in an RF plasma system, the composition of the plasma gas and the operating pressure have significant effects on the kinetics of fullerene formation [39]. Wang et al. [40] observed that synthesis in the pressure range of 19–65 kPa favored the formation of fullerenes. On the contrary, Cota-Sanchez [38] found that a pressure as low as 40 kPa was disadvantageous for fullerene formation. A similar result was found by Kim et al. [39] from their 2D numerical model simulations.

The main purpose of this study was to clarify the effect of metallic (Fe, Cu, Ni, Co, Ti) and non-metallic (Si, B) additives on fullerene formation. For Fe, Ni, Si, and B, the results were compared with the published ones. We could not find experimental data on the effect of Cu, Co, and Ti so far on fullerene synthesis in the RF thermal plasma condition.

To clarify the contradictory results on pressure dependence published earlier, we performed experiments on the effect of the operating pressure on the overall yield of fullerenes at pressures of 50, 72, and 92 kPa, respectively.

2. Results and Discussion

The synthesis conditions and the results of the product characteristics, such as the fullerene content of the soot and the C₇₀/C₆₀ ratio, are summarized in Table 1.

Table 1. Experimental parameters and the results of fullerene production in RF plasma.

Run	Additive (wt%)	Feed Rate (g·h ⁻¹)	E _{spec} (kWh·g ⁻¹)	Evaporation Ratio (%)	C ₇₀ /C ₆₀ Ratio	T _{vib-rot} (K)	Fullerene Content (wt%)
1	-	19	1.47	78	0.269	4500	5.1
2	Fe (5)	13	2.15	71	0.261	-	4.2
3	Fe (5)	46	0.61	72	0.259	-	3.9
4	Fe (20)	17	1.65	74	0.277	5100	6.2
5	Cu (20)	23	1.21	73	0.281	4000	5.5
6	Ni (20)	21	1.33	71	0.282	5800	4.3
7	Co (20)	22	1.27	70	0.288	5600	4.4
8	Ti (20)	22	1.27	59	0.465	4600	2.5
9	Si (5)	33	0.85	34	0.307	3900	3.3
10	B (5)	12	2.33	63	0.332	4500	1.2
11	Cu (5)	44	0.64	66	0.271	3900	3.2

The amount of additives was set to 5 or 20 wt% of the graphite powder. The feed rate of the mixtures varied in the range of 12–46 g·h⁻¹. Although the plate power was constant (28 kW) in all runs, the specific energy (E_{spec}; kWh·g⁻¹), defined as the energy applied for one gram of the precursor powder, varied in a wide range between 0.61 and 2.33 kWh·g⁻¹.

The experiments in the presence of 20 wt% Fe, 20 wt% Cu, 20 wt% Ti, 5 wt% Si, and 5 wt% B additives and without additives were repeated at least 2 times.

The addition of 5 wt% iron powder to the pure graphite reduced somewhat the fullerene content of the soot. However, in the presence of 20 wt% Fe, the fullerene content

of the soot increased significantly, which is in line with the findings of Cota-Sanchez [35]. They also found that a further increase in the iron content did not improve the fullerene yield, which made us set the upper limit of the additives as 20 wt% in our tests.

Copper (20 wt%) also has some positive effects on fullerene synthesis as compared to synthesis without additives, increasing the fullerene content of the soot. In contrast, no catalytic effect was detected in the presence of Ni and Co, although the mean particle size of these metal particles was optimal for plasma evaporation. The addition of Ti, Si, and B decreased significantly the fullerene content of the soot. In our synthesis conditions with Si addition to the graphite powder, we did not observe a positive effect on fullerene synthesis, as published by Wang [34]. This contradiction with Wang's results could be ascribed to several factors, including the a tenfold increase in the Si "additive" (~50 wt%) they employed or the lower pressure in the reactor chamber (150 torr/20 kPa). The latter resulted in a higher risk of oxygen infiltration, while the higher Si additive allegedly eliminated the oxidation of the carbon atoms. In the present tests, however, the pressure was close to atmospheric. As far as B is concerned, the results of this work are in agreement with those of Lange et al. [37].

The effect of copper was tested even with waste graphite powder from a turnery process. In spite of its high particle size, the fullerene content of the Cu-containing soot was a bit lower than that of pure graphite soot, but higher than in the case of B and Ti.

Solvents other than the typically used toluene, such as fullerenes, can be extracted in larger quantities than the amounts presented in Table 1. Extraction efficiency varies with the solvent type, where the choice of solvent is based on the solubility of fullerenes. Several solvents exhibit higher fullerene solubility (ortodichlorobenzene 27 mg/mL, phenylnaphtalene 50 mg/mL, cloronaphtalene 51 mg/mL) than observed for toluene (2.8 mg/mL) and, therefore, offer the prospect of improved extraction efficiency [13,41–43]. The extraction and the fullerene content were determined using ortodichlorobenzene (ODCB) for the soot obtained in the presence of 20 wt% Fe. The measured (6.9 wt%) value was slightly higher than that obtained with the toluene extraction (6.2 wt%). The analysis of the soot by single-photon ionization mass spectrometry indicated that there were several types of fullerenes, which were not found among the fullerenes extracted by typical solvents such as toluene, xylene, or o-dichlorobenzene, suggesting that they are readily incorporated into toluene-insoluble (xylene, o-dichlorobenzene) fullerene polymers. These "insoluble" fullerenes include isolated pentagon isomers of C_{74} (D3h) and many larger fullerenes, such as C_{78} -D'3h and C_{80} -Ih, and essentially all of the isomers of fullerenes with more than about 100 carbon atoms [44].

According to Cota-Sanchez [35], the intensive UV radiation of the plasma in the presence of metal vapors results in some photocatalytic effect, which may increase the fullerene content of the soot. For Fe addition, we observed a similar effect. However, in the presence of Ni and Co, there were no favorable effects of metal addition, in spite of intense UV radiation of particular metals in thermal plasma conditions. Due to the vaporization of graphite, carbon species such as C, C_2 , and C_3 are present in the plasma flame. It is generally accepted [38] that C_2 radicals play an important role in the process of fullerene formation under the plasma condition.

The recorded optical emission spectra were characterized by the dominance of the C_2 Swan system and atomic lines (argon and additive ones). Figure 1 shows the typical emission spectra of the C_2 radical. The vibration-rotation temperatures of the C_2 molecule were determined using diatomic line strength files for the Swan bands and a least-squares fitting algorithm [45,46].

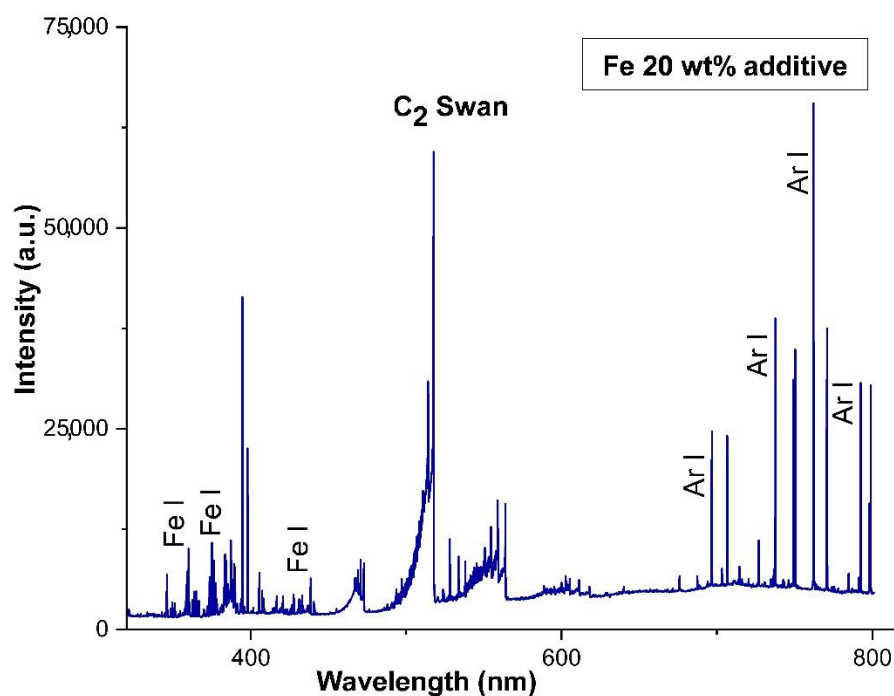


Figure 1. Emission spectrum of RF thermal carbon plasma in the presence of the iron additive.

In most cases, the fullerene content of the soot can be related to the extent of evaporation, which supports the importance of the C₂ concentration in the reactor. The evaporation ratio is defined as the volume percent of particles having diameters lower than 1 μm related to the total volume of particles, calculated from the particle size distribution of the soot. It can be regarded as a parameter characterizing the solid–gas heat and mass transfer in particular conditions. The scanning electron micrograph of the fullerene soot from Run 4 shows unevaporated graphite flakes surrounded by nanosized soot particles (Figure 2).

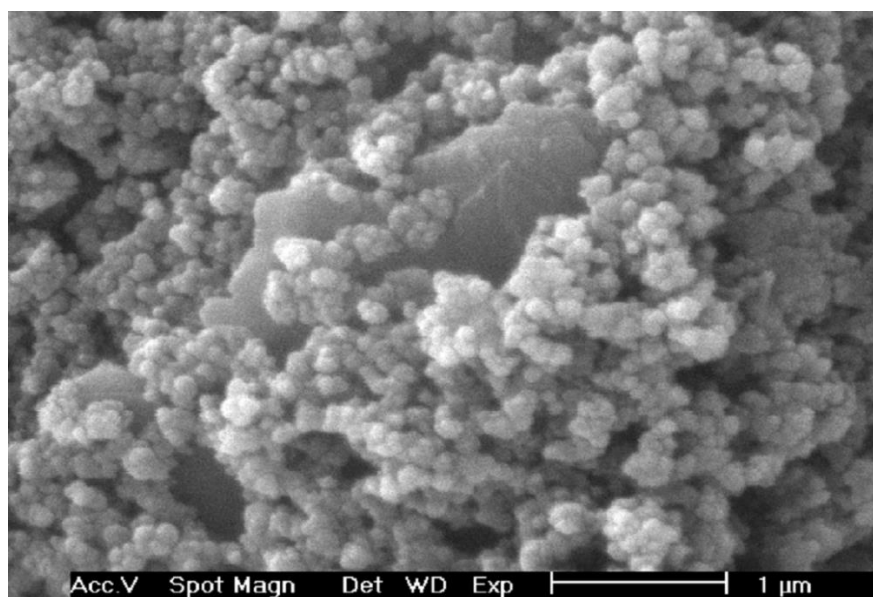


Figure 2. SEM photo of the soot obtained from Run 4.

Evaporation was similar for the pure graphite and the Fe- and Cu-containing starting materials (Runs 1, 2, 3, 4, 5). However, it was slightly lower in the case of the boron and

titanium additives (Run 8, 10). The presence of Si in the precursor (Run 9) decreased the extent of evaporation significantly.

Although the waste graphite powder had a higher mean particle size (D_{50} : 37 μm) than the reference graphite powder (D_{50} = 2.8 μm), their evaporation ratio was similar. While the original graphite particles could be identified in the soot obtained in Run 1 (pure graphite), they could not be detected using Run 11 (waste graphite precursor).

The specific energy ($\text{kWh}\cdot\text{g}^{-1}$) varied in the range of 0.61–2.33. The evaporation ratio was seemingly not affected by its actual value (Table 1). In Runs 2 and 3, the same precursor powder was fed with different feed rates. Despite the difference in the specific energies, the evaporation ratio was similar. Total evaporation was not observed even at a high Espec. This can be explained by the cohesive nature of the graphite powder. Precursor particles may form agglomerates that have too big a size to be heated to their sublimation temperature within the short residence time in the plasma flame.

The fullerene content is plotted against the extent of evaporation in Figure 3. For the Si case, higher, while, for the B case, lower fullerene content was detected, as compared to other cases. This refers to the presence of other effects in addition to the C_2 concentration in particular cases.

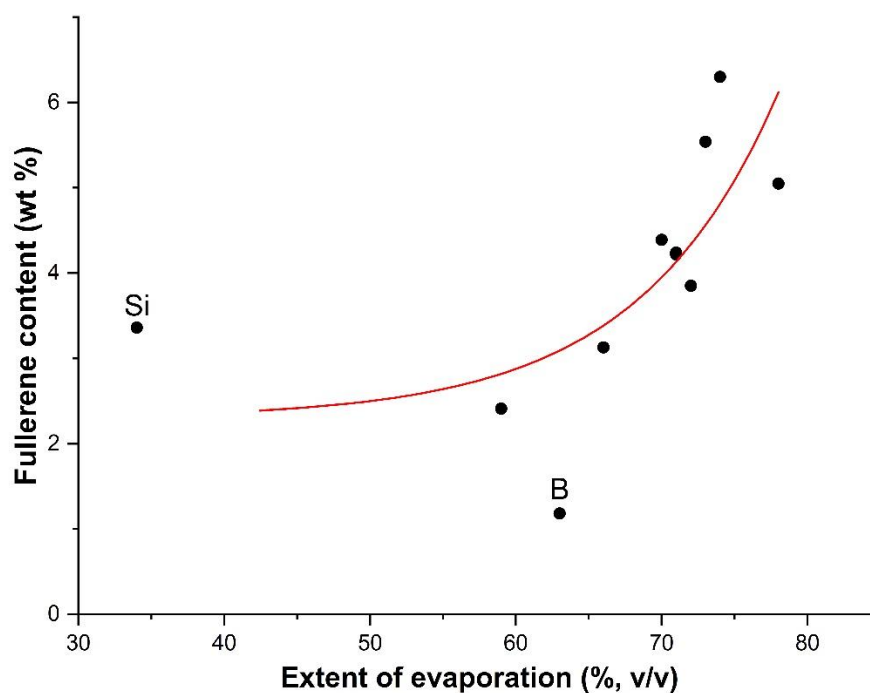


Figure 3. Fullerene content of the soot samples related to the extent of evaporation.

The crystalline structure of the soot from different runs (Run 4, 5, 6, 7, 8) was characterized by XRD. The carbonaceous soot obtained was used directly. The main phase in all reaction products was graphite and amorphous carbon (Figure 4). The patterns did, however, show a few additional lines, which could be attributed to metallic and oxidized metal precursors. In the presence of the Co precursor, peaks of unreacted Co and characteristic peaks of Co_3O_4 were detected. In Run 5, beyond the carbon phases, copper and oxidized copper were found both as Cu_2O and CuO . For the iron catalyst (Run 4), the synthesized powder consisted of Fe (C) phase reflexes such as αFe (C) and γFe (C). The XRD patterns of soot obtained with the Ti precursor (Run 8) contained, in addition to carbon phases, a smaller amount of oxidized titanium detected in a Ti_6O form. A significant quantity of TiC was also detected in this sample.

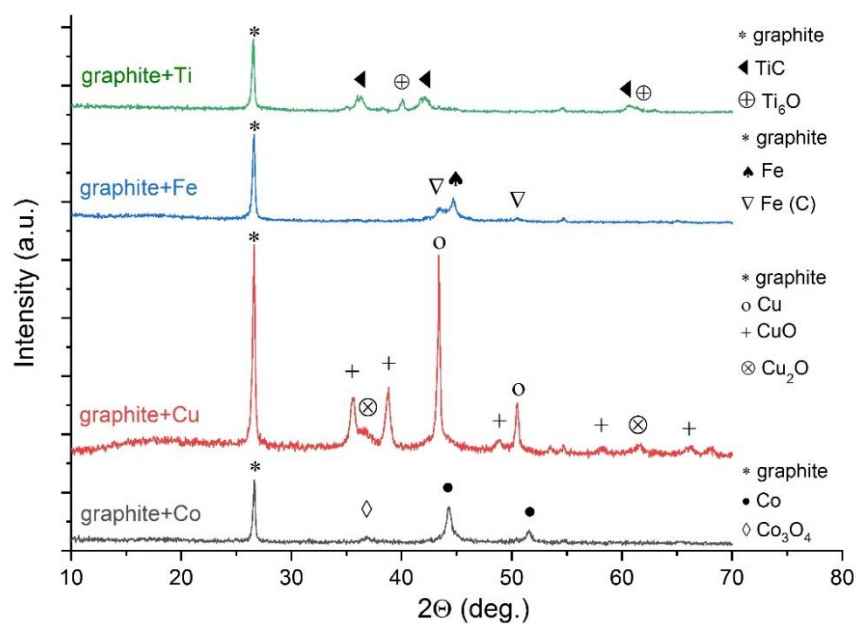


Figure 4. XRD pattern of the products of the particular runs with metal additives.

The effect of the additives on the fullerene composition was studied by HPLC measurements.

Chromatograms of the toluene extracts and assignment of the peaks are shown in Figure 5a,b. Due to its high UV absorption at 330 nm, C₆₀ was detected at 525 nm, while the other fullerenes were measured at 330 nm. Two major peaks (peak 1: C₆₀ and peak 2: C₇₀) and several smaller peaks (4, 5, 7, and 8) that can be assigned to higher fullerenes (C₇₆, C₇₈, C₈₄, and C₈₆) were detected. Smaller peaks at a retention time of about 35–45 min were not identified in the absence of available standard material. The fullerene compositions of the samples were estimated by comparing the normalized HPLC peak areas measured at 330 nm. Thus, this resulted in data for C₇₀ and higher fullerenes, as C₆₀ was detected at 525 nm.

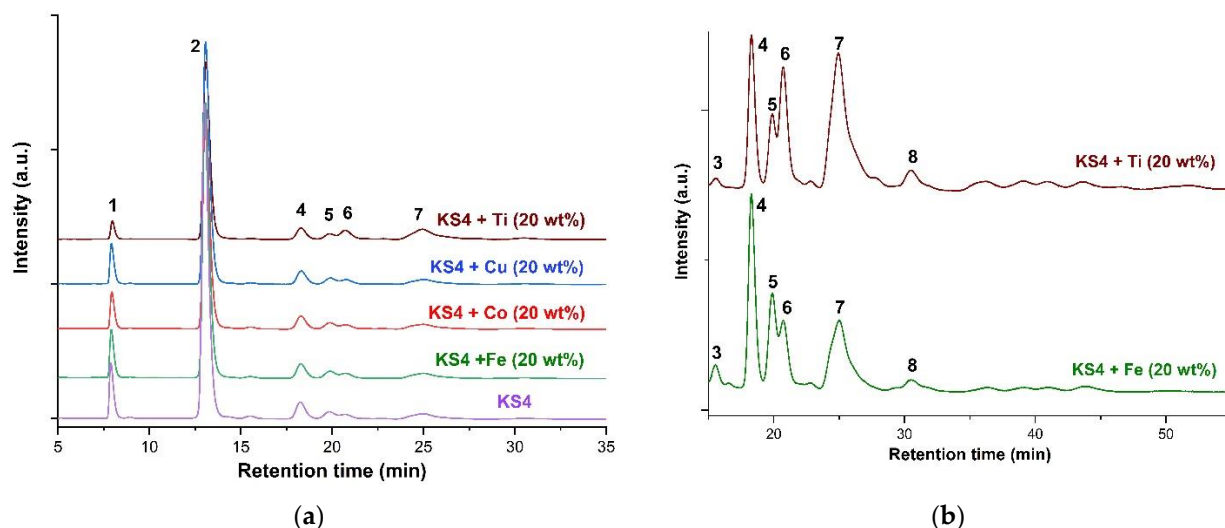


Figure 5. HPLC results of the toluene extracts for particular runs (a) with a 5–35 min retention time and (b) for runs with the Ti and Fe additives using a 15–55 min retention time. Assignment of peaks: 1: C₆₀, 2: C₇₀, 3: C₇₀O, 4: C₇₆, 5: C₇₈, 6: C₈₂, 7: C₈₄, 8: C₈₆.

The fullerene compositions were similar almost in all cases, except the titanium and boron additives. In the presence of Ti and B, the peaks corresponding to the C₈₂ and

C_{84} fullerenes were much higher than in the other samples (Figure 6). To emphasize the difference in composition, the peak areas corresponding to higher fullerenes (C_{76} , C_{78} , C_{82} , C_{84} , C_{86}) are shown in Figure 6. It can be seen that the presence of B and Ti facilitated the formation of higher fullerenes. Soot from the Ti, Si, and B cases showed a higher C_{70}/C_{60} ratio compared to other products (Table 1) as well.

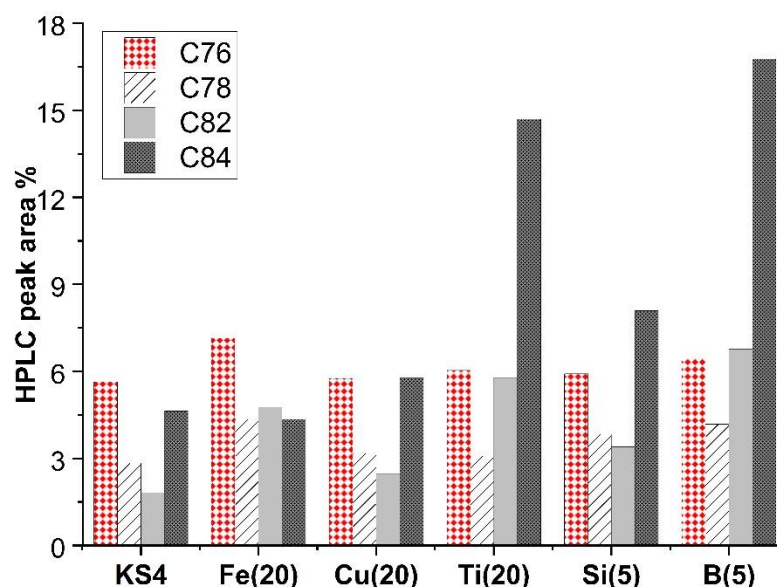


Figure 6. Comparison of higher fullerene (C_{76} , C_{78} , C_{82} , C_{84}) compositions in the presence of various additives.

In all our experiments, the C_{70} concentration (C_{70}/C_{60} ratio) produced was much higher (0.25–0.46) than predicted from equilibrium calculations (0.002) in atmospheric pressure [38].

This result supports the assumption of fullerene growth under non-equilibrium thermal conditions [38].

Gas phase synthesis from metal and carbon precursors is known to yield too many types of metal–carbon nanoclusters. Thus, it can be assumed that heterofullerenes, such as $C_{59}B$ and $C_{54}B_6$ [33], in the presence of the B additive and Ti_8C_{12} in the presence of Ti could be formed [47], but they could not be detected by the applied HPLC method, as they are not soluble in toluene.

The analysis of the effect of the reactor pressure on the concentration of extractable fullerenes revealed that at a higher system pressure (92 kPa), more fullerenes were formed both without and with the Cu additive (Table 2). At a low pressure (50 kPa), the fullerene content of the soot decreased to 0.1 wt%. Our results are in agreement with the results of thermodynamic calculations [38]. This can be explained by the longer mean residence time of carbon particles in the higher temperature region and, thus, their more intense evaporation. This led to an increased C_2 concentration in the gas phase.

Table 2. Fullerene yield for carbon and Cu-carbon systems at different operating pressures.

Pressure (kPa)	Fullerene Content %	
	No Additive	Cu Additive
50	0.1	0.1
72	1.7	1.5
92	5.05	5.54

In some of the cases (Run 1, 3, 4, 5, 9, and 10), the stability of the fullerenes in ambient air was tested. The results are summarized in Table 3. Toluene extractions were performed

just after synthesis and in 7 and 30 days, respectively. During this period, they were stored as solid materials in darkness. The fullerene content of the soot drastically decreased after storage of 7 days. In most samples, after 30 days, half of the extractable fullerenes disappeared from the soot with the exception of boron, where 80% of the fullerenes remained in the soot (Run 10). In this case, the fullerenes had higher stability in the soot compared to the other samples.

Table 3. Stability of fullerene soot over time.

Additive (wt%)	Fullerene Content %		
	0 Days	7 Days	30 Days
-	5.05	3.38	2.47
Fe (5)	4.22	3.37	2.53
Fe (20)	6.30	4.28	3.213
Cu (20)	5.54	3.87	2.65
Si (5)	3.36	2.35	1.78
B (5)	1.18	1.10	0.94

Further investigations are needed to determine whether fullerenes form non-extractable oligomers with time or transform into the graphite structure.

3. Materials and Methods

Pure graphite powder (KS4, Timcal Co., Bodio, Switzerland, with a mean particle size $D_{50} = 2.8 \mu\text{m}$), and its mixtures with metallic and non-metallic additives including Fe (D_{50} : 35 μm), Cu (D_{50} : 45 μm), Co (D_{50} : 5 μm), Ni (D_{50} : 5 μm), Ti (D_{50} : 45 μm), Si (D_{50} : 14.9 μm), and B (D_{50} : 28.2 μm) powders, respectively, were subjected to thermal plasma treatment in an RF plasma system (3–5 MHz, PL-35 torch (TEKNA Ltd., Sherbrooke, Canada)) [31]. In one case, a copper-containing waste graphite powder (D_{50} : 37 μm) from the turnery process was used as the precursor as well. The graphite powders were injected axially to the top of the plasma flame with feed rates of 12–50 $\text{g}\cdot\text{h}^{-1}$ at a plate power of 28 kW and a pressure of 92 kPa. In all the runs, the gas flow rates and the plate power were set to constant values as follows: plasma gas 8 Ar + 8.5 He slpm; sheath gas 12 Ar + 28 He slpm; carrier gas 6 He slpm. The role of the He was to improve the heat conductivity and the enthalpy of the plasma. Thus, higher heating rates and, most probably, higher reaction temperatures are achieved in its presence, which facilitates the evaporation of solid particles.

The optimal experimental conditions for this setup were determined for graphite powders without additives and published in a former paper [33].

Pressure-dependent experiments were performed at 50, 72, and 92 kPa with graphite without additives and repeated in the presence of Cu as well.

The emission of the plasma was detected through a quartz glass window at a distance of 15 cm from the bottom of the plasma nozzle. The wavelength was selected by a 55 cm focal length monochromator (TRIAX 550 Jobin-Yvon, Horiba, Montpellier, France). Gratings with 300 and 1200 grooves/mm were used. Light was collected and transferred to the entrance slit by fiber optics. Plasma emission was detected by an optical multi-channel analyzer (CCD-3000, Jobin-Yvon, Horiba, Montpellier, France). The available spectral range was between 300 and 1000 nm.

The main reaction product was solid soot collected from the water-cooled reactor wall at the same distance along the reactor axis (30–50 cm from the plasma torch). Fullerene soots were characterized by their particle size distribution, measured with the laser diffraction technique using a Malvern Mastersize 2000, Malvern Pananalytical Ltd., Malvern, United Kingdom, and their morphology by scanning electron microscopy (SEM, Philips XL30 ESEM, Amsterdam, Netherlands), and a composition using X-ray powder diffraction (XRD) was performed. The XRD patterns were obtained with a Philips instrument PW 3710 equipped with a PW 1050 Bragg–Brentano parafocusing goniometer, using monochromatized Cu Ka radiation. The XRD scans were digitally recorded with steps of

0.041 in the 2 h range from 4° to 80°. The quantitative phase composition was evaluated using a full profile fit method with corrections for preferred orientation and micro absorption [48]. To separate fullerenes, the soot was extracted by toluene at a 100 mg solid/10 mL liquid ratio for one minute at 20 °C. The amount of fullerenes was measured by a UV-VIS spectrophotometer against C₆₀-containing reference solutions. The first extraction was undertaken on the day of the synthesis, and the time-dependent stability was measured by repeating the extraction after 7 days and 30 days. The fullerene composition was measured by the HPLC technique (LSS-1500, Jasco Int. Co., Tokyo, Japan), with a UV/visible detector and analytical Cosmosil Buckyprep column.

4. Conclusions

Additives influence both the fullerene content and the fullerene composition of the soot and help or hinder the decomposition or transformation of the cage structures in the soot with time.

Iron and copper catalyzed fullerene formation in the RF plasma condition, however only when the metallic additives were present in a higher weight ratio (20%). Ni, Co, and Ti showed no catalytic effect on fullerene formation even at a high concentration. On the contrary, the total fullerene yield abruptly dropped in the presence of Ti. It was demonstrated, however, that Ti promoted the formation of higher fullerene clusters such as C₈₂, C₈₄, and C₈₆, and the ratio of C₇₀/C₆₀ in the soot was also higher than in the cases of other metallic additives.

Copper definitely facilitated the evaporation of the graphite powder. At the present level of our knowledge, we can assume that the metal-containing graphite powders from the turnery process can be used as precursors for fullerene production in RF thermal plasma. Thus, a high-value product can be synthesized from hazardous waste.

Non-metallic additives such as Si and B reduced the formation of fullerenes in the RF plasma condition, and both of them showed similar effects as Ti regarding the changes in the fullerene composition: the ratio of higher fullerenes (C₈₂, C₈₄, and C₈₆) increased at the expense of lower fullerenes as compared to the other samples. However, the proportion of C₆₀ and C₇₀ still comprised the greatest part of the fullerenes, while the C₇₀/C₆₀ ratio was also higher than without additives. Among the products, amorphous carbon and graphite precursor residues were also found in smaller quantities. In the presence of titanium, a significant quantity of TiC was also formed as a by-product.

The stability of solid fullerenes adsorbed on the soot was not influenced by the presence of Fe, Cu, and Si upon storage. In 30 days, the soot from the pure, the Fe-, the Cu-, and the Si-doped graphites lost 40–50% of their original fullerene content. As a novel finding, it was shown that the boron additive may inhibit the decomposition of the cage structures in the soot in solid form during storage in ambient air. The possible mechanism of this effect must be clarified in future tests.

It was experimentally proven that a higher reactor pressure improves the fullerene yield in RF plasma conditions.

Author Contributions: Conceptualization, A.M.K. and J.S.; methodology, E.B. and É.K.; investigation, A.M.K., E.B. and É.K.; writing—original draft preparation, A.M.K.; writing—review and editing, A.M.K. and Z.K.; visualization, A.M.K.; supervision, Z.K.; project administration, J.S.; funding acquisition, J.S. All authors have read and agreed to the published version of the manuscript.

Funding: This research received no external funding.

Institutional Review Board Statement: Not applicable.

Informed Consent Statement: Not applicable.

Data Availability Statement: Not applicable.

Acknowledgments: The authors are indebted to Ilona Mohai for her assistance and initiation of the topic. Eszter Bódis acknowledges financial support from the János Bolyai Research Scholarship from the Hungarian Academy of Sciences.

Conflicts of Interest: The authors declare no conflict of interest.

References

1. Kroto, H.W.; Heath, J.R.; O'Brien, S.C.; Curl, R.F.; Smalley, R.E. C₆₀: Buckminsterfullerene. *Nature* **1985**, *318*, 162–163. [[CrossRef](#)]
2. Guldi, D.M.; Illescas, B.M.; Atienza, C.M.; Wielopolskia, M.; Martin, N. Fullerene for organic electronics. *Chem. Soc. Rev.* **2009**, *38*, 1587–1597. [[CrossRef](#)] [[PubMed](#)]
3. Dennler, G.; Scharber, M.C.; Brabec, C.J. Polymer-Fullerene Bulk-Heterojunction Solar Cells. *Adv. Mater.* **2009**, *21*, 1323–1338. [[CrossRef](#)]
4. Alsulam, I.K.; Alharbi, T.M.; Moussa, M.; Raston, C.L. High-Yield Continuous-Flow Synthesis of Spheroidal C₆₀@ Graphene Composites as Supercapacitors. *ACS Omega* **2019**, *4*, 19279–19286. [[CrossRef](#)] [[PubMed](#)]
5. Ramezanitaghartapeh, M.; Achazi, A.J.; Soltani, A.; Miró, P.; Mahon, P.J.; Hollenkamp, A.F.; Musameh, M. Sustainable cyanide-C₆₀ fullerene cathode to suppress the lithium polysulfides in a lithium-sulfur battery. *Sustain. Mater. Technol.* **2022**, *32*, e00403. [[CrossRef](#)]
6. Shetti, N.P.; Mishra, A.; Basu, S.; Aminabhavi, T.M. Versatile fullerenes as sensor materials. *Mater. Today Chem.* **2021**, *20*, 100454. [[CrossRef](#)]
7. Aoyagi, S.; Nishibori, E.; Sawa, H.; Sugimoto, K.; Takata, M.; Miyata, Y.; Kitaura, R.; Shinohara, H.; Okada, H.; Sakai, T.; et al. A layered ionic crystal of polar Li@C(60) superatoms. *Nat. Chem.* **2010**, *2*, 678–683. [[CrossRef](#)]
8. Todorović Marković, B.; Jokanović, V.; Jovanović, S.; Kleut, D.; Dramićanin, M.; Marković, Z. Surface chemical modification of fullerene by mechanochemical treatment. *Appl. Surf. Sci.* **2009**, *255*, 7537–7541. [[CrossRef](#)]
9. Pilehvar, S.; De Wael, K. Recent Advances in Electrochemical Biosensors Based on Fullerene-C₆₀ Nano-Structured Platforms. *Biosensors* **2015**, *5*, 712–735. [[CrossRef](#)]
10. Wudl, F. Fullerene materials. *J. Mater. Chem.* **2002**, *12*, 1959–1963. [[CrossRef](#)]
11. Maruyama, H.; Tomonoh, S.; Alford, J.M.; Karpuk, M.E. Fullerene Production in Tons and More: From Science to Industry. *Fuller. Nanotub. Carbon Nanostruct.* **2005**, *1*, 1–9. [[CrossRef](#)]
12. Gruenberger, T.; Probst, N.; Fulcheri, L. Fullerene and carbon nanoparticle production via continuous AC plasma process. *Chimica Oggi* **2004**, *22*, 48–51. [[CrossRef](#)]
13. Keypour, H.; Noroozi, M.; Rashidi, A. An improved method for the purification of fullerene from fullerene soot with activated carbon, celite, and silica gel stationary phases. *J. Nanostruct. Chem.* **2013**, *3*, 45–51. [[CrossRef](#)]
14. Kyesmen, P.I.; Onoja, A.; Amah, A.N. Fullerenes synthesis by combined resistive heating and arc discharge techniques. *Chem. SpringerPlus* **2016**, *5*, 1–7. [[CrossRef](#)]
15. Kratschmer, W.; Lamb, L.D.; Fostiropoulos, K.; Huffman, D.R. Solid C₆₀: A new form of carbon. *Nature* **1990**, *347*, 354–358. [[CrossRef](#)]
16. Lange, A.; Huczko, A. Influence of nitrogen on carbon arc plasma and formation of fullerenes. *Chem. Phys. Lett.* **2001**, *340*, 1–6. [[CrossRef](#)]
17. Churilov, G.N. Synthesis of fullerenes and other nanomaterials in arc discharge Fullerenes. *Nanotub. Carbon Nanostruct.* **2008**, *16*, 395–403. [[CrossRef](#)]
18. Kareev, I.E.; Nekrasov, V.M.; Buhnov, V.P. Electric-arc synthesis of soot with a high content of higher fullerenes. *Tech. Phys.* **2015**, *60*, 102–106. [[CrossRef](#)]
19. Chibante, L.P.F.; Thess, A.; Alford, J.M.; Diener, M.D.; Smalley, R.E. Solar generation of the fullerenes. *J. Phys. Chem.* **1993**, *61*, 8696–8700. [[CrossRef](#)]
20. Mordkovich, V.Z.; Shiratori, Y.; Hiraoka, H.; Takeuchi, Y. Synthesis of multishell fullerenes by laser vaporization of composite carbon targets. *Phys. Solid State* **2002**, *44*, 603–606. [[CrossRef](#)]
21. Todorovic-Markovic, B.; Markovic, Z.; Mohai, I.; Nikolic, Z.; Farkas, Z.; Szépvölgyi, J. Influence of Carbon Concentration and Rotational Temperature on Fullerene Yield in RF Reactor. *Mater. Sci. Forum* **2006**, *518*, 211–216. [[CrossRef](#)]
22. Todorovic-Markovic, B.; Markovic, Z.; Mohai, I.; Károly, Z.; Gál, L.; Föglein, K.; Szabó, P.T.; Szépvölgyi, J. Efficient synthesis of fullerenes in RF thermal plasma reactor. *Chem. Phys. Lett.* **2003**, *378*, 434–439. [[CrossRef](#)]
23. Yoshie, K.; Kasuya, S.; Eguchi, K.; Yoshida, T. Novel method for C₆₀ synthesis: A thermal plasma at atmospheric pressure. *Appl. Phys. Lett.* **1992**, *61*, 2782–2783. [[CrossRef](#)]
24. Howard, J.B.; Mckinnon, J.T.; Makarovskiy, Y.; Lafleur, A.L.; Johnson, M.E. Fullerenes C₆₀ and C₇₀ in flames. *Nature* **1991**, *352*, 139–142. [[CrossRef](#)]
25. Takehara, H.; Fujiwara, M.; Arikawa, M.; Diener, M.D.; Alford, J.M. Experimental study of industrial scale fullerene production by combustion synthesis. *Carbon* **2005**, *43*, 311–319. [[CrossRef](#)]
26. Alford, J.M.; Diener, M.D.; Nability, J.; Karpuk, M. Burners and combustion apparatus for carbon nanomaterial production. US Patent 72792317, 9 October 2007.
27. Alford, J.M.; Bernal, C.; Cates, M.; Diener, M.D. Fullerene production in soothing flames from 1,2,3,4-tetrahydronaphthalene. *Carbon* **2008**, *46*, 1623–1625. [[CrossRef](#)]
28. Amsharov, K.Y.; Jansen, M. A C₇₈ Fullerene Precursor: Toward the Direct Synthesis of Higher Fullerenes. *J. Org. Chem.* **2008**, *73*, 2931–2934. [[CrossRef](#)]

29. Otero, G.; Giulio, G.; Sánchez-Sánchez, B.C.; Caillard, R.; López, M.F.; Rogero, C.; Palomares, F.J.; Cabello, N.; Basanta, M.A.; Ortega, J.; et al. Fullerenes from aromatic precursors by surface-catalysed cyclodehydrogenation. *Nature* **2008**, *454*, 865–868. [[CrossRef](#)]
30. Kabdulov, M.A.; Amsharov, K.Y.; Jansen, M. A step toward direct fullerene synthesis: C60 fullerene precursors with fluorine in key positions. *Tetrahedron* **2010**, *66*, 8587–8593. [[CrossRef](#)]
31. Viñes, F.; Görling, A. Template-Assisted Formation of Fullerenes from Short-Chain Hydrocarbons by Supported Platinum Nanoparticles. *Angew. Chem. Int. Ed.* **2011**, *50*, 4611–4614. [[CrossRef](#)]
32. Marković, Z.; Todorović-Marković, B.; Mohai, I.; Farkas, Z.; Kovats, E.; Szepvolgyi, J.; Otašević, D.; Scheier, P.; Feil, S.; Romčević, N. Comparative Process Analysis of Fullerene Production by the Arc and the Radio-Frequency Discharge Methods. *J. Nanosci. Nanotechnol.* **2007**, *7*, 1357–1369. [[CrossRef](#)]
33. Szepvolgyi, J.; Marković, Z.; Todorović-Marković, B.; Nikolic, Z.; Mohai, I.; Farkas, Z.; Tóth, M.; Kováts, E.; Scheier, P.; Feil, S. Effects of precursors and plasma parameters on fullerene synthesis in RF thermal plasma reactor. *Plasma Chem. Plasma Proc.* **2006**, *26*, 597–608. [[CrossRef](#)]
34. Wang, C.; Imahori, T.; Tanaka, Y.; Sakuta, T.; Takikawa, H.; Matsuo, H. Silicon inclusion effect on fullerene formation under induction thermal plasma condition. *Thin Solid Films* **2002**, *407*, 72–78. [[CrossRef](#)]
35. Cota-Sanchez, G.; Soucy, G.; Huczko, A.; Beauvais, J.; Drouin, D. Effect of Iron Catalyst on the Synthesis of Fullerenes and Carbon Nanotubes in Induction Plasma. *J. Phys. Chem. B* **2004**, *108*, 19210–19217. [[CrossRef](#)]
36. Guo, T.; Jin, C.M.; Smalley, R.E. Doping Bucky: Formation and Properties of Boron-Doped Buckminsterfullerene. *J. Phys. Chem.* **1991**, *95*, 4948–4950. [[CrossRef](#)]
37. Lange, H.; Huczko, A.; Byszewski, P.; Mizera, E.; Shinohara, H. Influence of boron on carbon arc plasma and formation of fullerenes and nanotubes. *Chem. Phys. Lett.* **1998**, *289*, 174–180.
38. Cota-Sanchez, G.; Soucy, G.; Huczko, A.; Lange, H. Induction plasma synthesis of fullerenes and nanotubes using carbon black–nickel particles. *Carbon* **2005**, *43*, 3153–3166. [[CrossRef](#)]
39. Kim, K.S.; Moradian, A.; Mostaghimi, J.; Soucy, G. Modeling of Induction Plasma Process for Fullerene Synthesis: Effect of Plasma Gas Composition and Operating Pressure. *Plasma Chem. Plasma Proc.* **2010**, *30*, 91–110. [[CrossRef](#)]
40. Wang, C.; Inazaki, A.; Shirai, T.; Tanaka, Y.; Sakuta, T.; Takikawa, H.; Matsuo, H. Effect of ambient gas and pressure on fullerene synthesis in induction thermal plasma. *Thin Solid Films* **2003**, *425*, 41–48. [[CrossRef](#)]
41. Törpe, A.; Belton, D.J. Improved Spectrophotometric Analysis of Fullerenes C60 and C70 in High-solubility Organic Solvents. *Anal. Sci.* **2015**, *31*, 125–130.
42. Kozlov, V.S.; Suyasova, M.; Lebedev, V.T. Synthesis, extraction, and chromatographic purification of higher empty fullerenes and endohedral gadolinium metallofullerenes. *Russ. J. Appl. Chem.* **2014**, *87*, 121–127. [[CrossRef](#)]
43. Tsetkova, L.V.; Keskinov, V.A.; Charykov, N.A.; Alekseev, N.I.; Gruzinskaya, E.G.; Semenov, K.N.; Postnov, V.N.; Krokhina, O.A. Extraction of fullerene mixture from fullerene soot with organic solvents. *Russ. J. Gen. Chem.* **2011**, *81*, 920–926. [[CrossRef](#)]
44. Raebiger, J.W.; Alford, J.M.; Bolskar, R.D.; Diener, M.D. Chemical redox recovery of giant, small-gap and other fullerenes. *Carbon* **2011**, *49*, 37–46. [[CrossRef](#)]
45. Parriger, C.G.; Plemmons, D.H.; Hornkohl, J.O.; Lewis, J.W.L. Spectroscopic temperature measurements in a decaying laser-induced plasma using the C2 Swan system. *J. Quant. Spectrosc. Radiat. Transfer.* **1994**, *52*, 707–711. [[CrossRef](#)]
46. Parriger, C.G.; Hornkohl, J.O.; Keszler, A.M.; Nemes, L. Measurement and analysis of atomic and diatomic carbon spectra from laser ablation of graphite. *Appl. Opt.* **2003**, *42*, 6192–6198.
47. Selvan, R.; Pradeep, T. Towards the synthesis and characterization of metallocarbohedrenes. *Chem. Phys. Lett.* **1999**, *309*, 149–156. [[CrossRef](#)]
48. Taylor, J.C. Computer Programs for Standardless Quantitative Analysis of Minerals Using the Full Powder Diffraction Profile. *Powder Diffr.* **1991**, *6*, 2–9. [[CrossRef](#)]